EFFICIENT REPRESENTATION OF REFLECTING STRUCTURES FOR A SONAR NAVIGATION MODEL

Roman Kuc* and M. W. Siegel**

* Department of Electrical Engineering, Yale University, New Haven, CT 06520

** The Robotics Institute, Carnegie-Mellon University, Pittsburgh, PA 15213

ABSTRACT

A physically-based simulation model for a sonar navigation system is described, in which the reflecting elements consist of walls, corners and edges arranged in a floor plan. When the transducer is operating in the pulse/echo mode, each element that falls in the transducer field-of-view contributes to the reflected signal through its impulse response. The floor plan is represented as a two-dimensional grid of visibels, that indicate which elements are visible from a particular location. A visibel is represented by a word in computer memory, each bit of which is assigned to a particular element (corner, wall or edge) in the floor plan. The advantage of this conceptually simple approach is that it allows the transducer to move through the floor plan efficiently. This efficiency results because the visibel values are set prior to signal generation, thus allowing a variety of transducer types or transducer locations to be examined quickly. Examples of simulated sonar maps using the time-of-flight ranging system are shown for two floor plans, one simple and the second more complicated. The simulations are verified by comparing them with actual sonar maps obtained with the Polaroid sensor.

INTRODUCTION

Acoustic sensors provide an inexpensive means for determining the proximity of objects and are commonly used for implementing sonar systems for mobile robot navigation [1,2,3]. One common implementation is the time-of-flight (TOF) system, which has been inexpensively packaged by the Polaroid Corporation [4]. An important consideration involving current sonar systems is that the observed waveforms are complex and require some assumptions to be interpreted. One set of such assumptions may be as follows: 1) if a TOF reading is produced, then an object must lie along the transducer line-of-sight at that range, and 2) if an object is present along the transducer line-of-sight, then a TOF reading will be produced. We illustrate in this paper that the validity of these assumptions is reasonable in some cases but, more often, they are inappropriate. The consequences in the latter case include the presence of artifacts in sonar maps and the absence of actual obstacles in robot navigation applications.

To provide a better understanding of sonar ranging, we implemented a simulation model that is based on the physical principles of sound propagation. Such a model has three important applications. First, the model should assist in the interpretation of observed TOF readings, leading to improved sonar maps. Second, by illustrating the various factors that contribute to the observed sonar signal, insights can be obtained toward achieving a more accurate solution to the inverse problem, than that offered by the TOF implementation. The third application is that this model may prove useful for developing navigation concepts without the need for much tedious experimentation with robot hardware.

In the next section, we review the principles of TOF ranging systems. In section 3, a simple physical interpretation for the reflection process from smooth surfaces is presented and applied to the reflections from walls, corners and edges. In section 4, we describe an efficient procedure to represent these elements in a floor plan. Simulated sonar maps are compared to actual data in section 5.

CURRENT ULTRASOUND RANGING SYSTEMS

Most ultrasound ranging systems currently employ a single acoustic transducer that acts as both a transmitter and receiver [5]. After the transmitted pulse encounters an object, an echo is detected by the same transducer acting as a receiver. An example of a typical echo is shown in Fig. 1. A conventional time-of-flight (TOF) system produces a range value corresponding to the time the echo amplitude exceeds a threshold level. This is shown to occur at time $t=t_o$ in Fig. 1. Time-controlled gain amplifiers are commonly employed to compensate for the spreading loss due to diffraction and attenuation in air [5]. Hence, the reflection amplitude can be considered to be independent of range.

A range measurement z_o is obtained from the round-trip time-of-flight by the following formula

$$z_o = ct_o/2 \qquad (1)$$

where c is the speed of sound in air (343 m/s at room temperature). A sonar map is generated by placing a dot at the measured range along the transducer line-of-sight. The transducer is then rotated to a new angle, another pulse is trans-

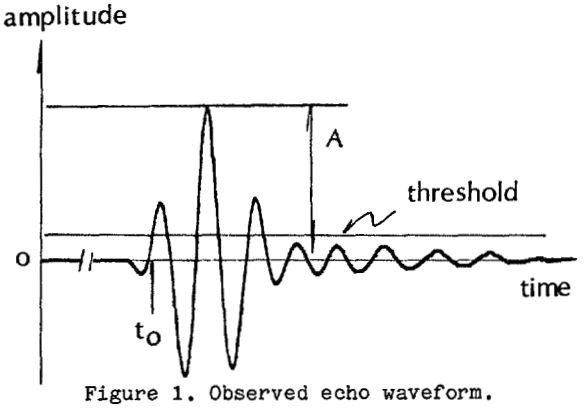

Figure 1. Observed echo waveform.

mitted and the process is repeated. When the transducer is rotated about a stationary point to take TOF readings at constant increments in angle, the resulting map is called a sector scan [5]. An equivalent map is produced when, instead of rotating the transducer, multiple transducers mounted in a ring are employed [1].

PHYSICALLY-BASED MODEL OF THE REFLECTION PROCESS

In this section, we present a physically-based model that describes the reflection process from smooth planes that act like mirrors. Such specular reflectors allow the transmitter/receiver transducer to be broken up into a separate transmitter and a virtual receiver. We then consider the signals scattered from the three components, corners, edges and walls, that populate our CEW world. Walls are simple planes, while corners and edges are located at the intersections of planes, as shown in Fig. 2.

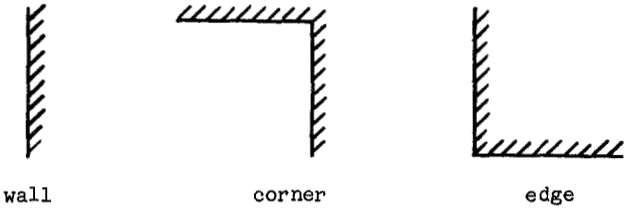

Figure 2. Elements in CEW world.

Corners are like walls in that they produce reflections, while edges produce diffracted signals that are detected at the receiver. These two cases are treated separately. To determine the interaction, or acoustic signature, of each of these elements, we consider the impulse response approach, in which the signal produced by the transmitter is an impulsive plane wave and the response is the signal scattered by the element and detected at the receiver [6]. The signals observed by an actual transducer are then equal to the convolution of this impulse response and the pulse waveform, an example of which was shown in Fig. 1.

Impulse responses of corners and walls. The reflected signals detected from walls and corners are specular in that the angle of the reflected wave with respect to the normal is equal to the angle of incident wave. Under this condition, the transmitter/receiver T/R can be broken up into a transmitting transducer T and a virtual receiver R', as shown in Fig. 3. The orientation of

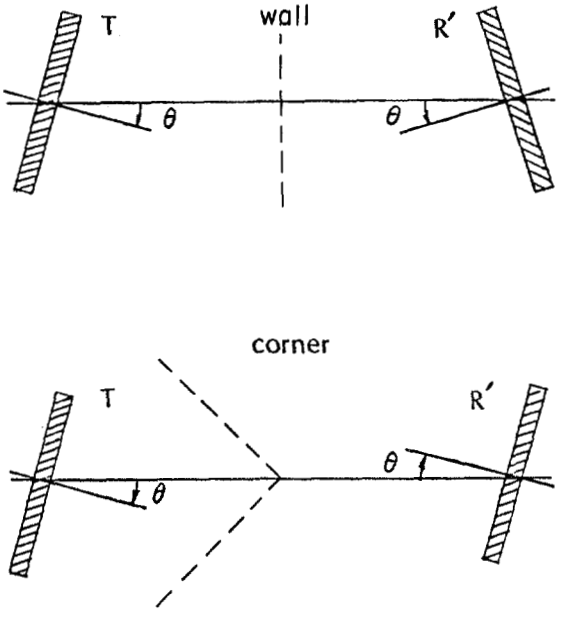

Figure 3. Mirror model of wall and corner.

the virtual receiver with respect to the transmitter can be determined by tracing rays from the edges of the transducer [6]. For the plane, we define the deviation from normal incidence as the inclination angle, denoted by θ. For the corner, θ is the angle of the line from the center of the transducer to the point defining the corner with respect to the transducer line-of-sight. For the corner, the inclination angle of the virtual receiver has the same magnitude but the opposite sign of that for the plane.

In the impulse response formulation, the transmitted signal is an impulsive plane wave. In the detection process, this plane wave sweeps across the receiver aperture. At normal incidence, or θ=0, this occurs instantaneously. For off-normal incidence, or θ≠0, the time for the plane wave to traverse the aperture is finite and increases with the magnitude of θ. For a circular aperture, the impulse response, denoted by $h(t,z,a,\theta)$, has a closed analytic form [6] equal to

$$h(t,z,a,\theta) = \frac{2c\cos\theta}{\pi a \sin|\theta|}\left(1-(ct-2z)^2\right)^{1/2}, \quad (2)$$

for $-\pi/2 \le \theta \le \pi/2$, $\theta \neq 0$, and for $\frac{2z-a\sin\theta}{c} \le t \le \frac{2z+a\sin\theta}{c}$

$$= \delta(t-2z/c), \text{ for } \theta=0,$$

where a is the radius of the aperture and $\delta(t)$ is the Dirac delta function. The $\cos\theta$ term arises because the transducer is sensitive only to the normally-incident pressure component.

From (2), we note that the form of the response does not depend on the sign of the inclination angle θ. Since the model for the corner differs from that of the wall in only the sign of θ, the two cannot be differentiated from the reflected signal. This is true when the transducer aperture is symmetric about the axis of rotation, as is the case for the circular aperture. The consequence of this statement is illustrated in the sonar maps generated below. A method to differentiate walls from corners by using two transducers is described in reference [7].

By reciprocity, the transmitter, when excited by an impulse, also has the same impulse response as the receiver. Hence, the impulse response of the transmitter/receiver pair, $h_{T/R}(t,z,a,\theta)$, is equal to the convolution of the two impulse responses given in (2), or

$$h_{T/R}(t,z,a,\theta) = \int_{(2z-a\sin\theta)/c}^{(2z+a\sin\theta)/c} h(\beta,z,a,\theta)\, h(t-\beta,z,a,\theta)\, d\beta. \quad (3)$$

The family of these T/R impulse responses with θ as a parameter is shown in Fig. 4.

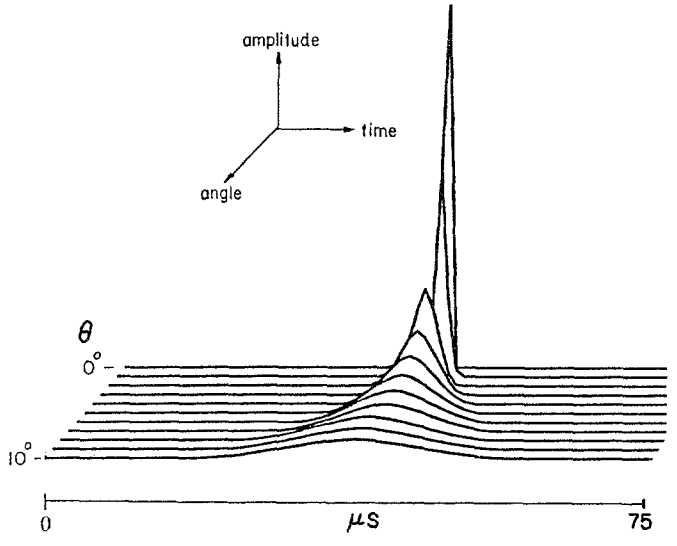

Figure 4. T/R impulse responses (a=20 mm).

The importance of the above result is that the impulse response is given in a closed analytic form that can be evaluated efficiently. The standard method for doing this employs the Huygen's principle argument of breaking the transmitter and receiver apertures into small elements and computing the interaction between all possible pairs.

Impulse response of an edge. The signal scattered from an edge is more complicated that those from the wall and corner. When a plane wave is incident on the line defining the edge, the signal that is detected by the receiver is from the diffracted signal. This signal is a cylindrical wave that appears to originate at the edge location, as shown in Fig. 5.

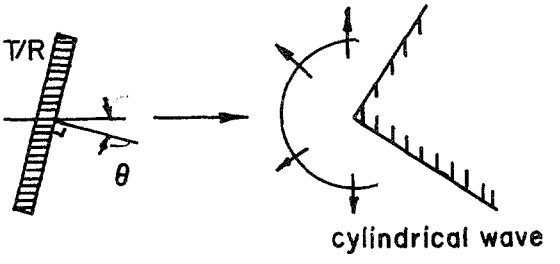

Figure 5. Model of the edge.

We use the results from acoustics [8] that describe the diffracted signal from a knife edge to approximate the impulse response of the edge, denoted by $h_E(t,z,a,\theta,\lambda)$. The result is given by

$$h_E(t,z,a,\theta,\lambda) = \frac{h_{T/R}(t,z,a,\theta)}{2\pi(z/\lambda)^{1/2}} \quad (4)$$

where $\lambda=c/f_R$, is the wavelength of the acoustic wave and f_R is the resonant frequency of the transducer [6]. The magnitude factor $2\pi(z/\lambda)^{-1/2}$ indicates the amplitude of the signal scattered from the edge relative to that of the reflection from a corner or wall. Otherwise, the form of this impulse response is identical to that for the wall and corner.

Generating a TOF dot. Equipped with the impulse responses described above, we can form a floor plan comprised of these elements and situate a transducer at any location within the interior space. The total response observed by the transducer is then equal to the sum of the responses of all the elements that are within the field-of-view of the transducer, equal to $\pm 90^\circ$ with respect to the line-of-sight. The procedure to generate a TOF range dot in a sonar map is illustrated in Fig. 6. In Fig. 6, the transmitter/receiver is shown with its line-of-sight indicated as a dashed line. The five elements that produce detectable reflections are numbered. All corners and edges lying within $\pm 90^\circ$ of the line-of-sight will produce detectable reflections, while walls in this space must have a section that is normally incident to the transducer. Each of these reflecting elements generates its own impulse response, whose time position is determined by its range from the transducer and its amplitude is determined by its angle of

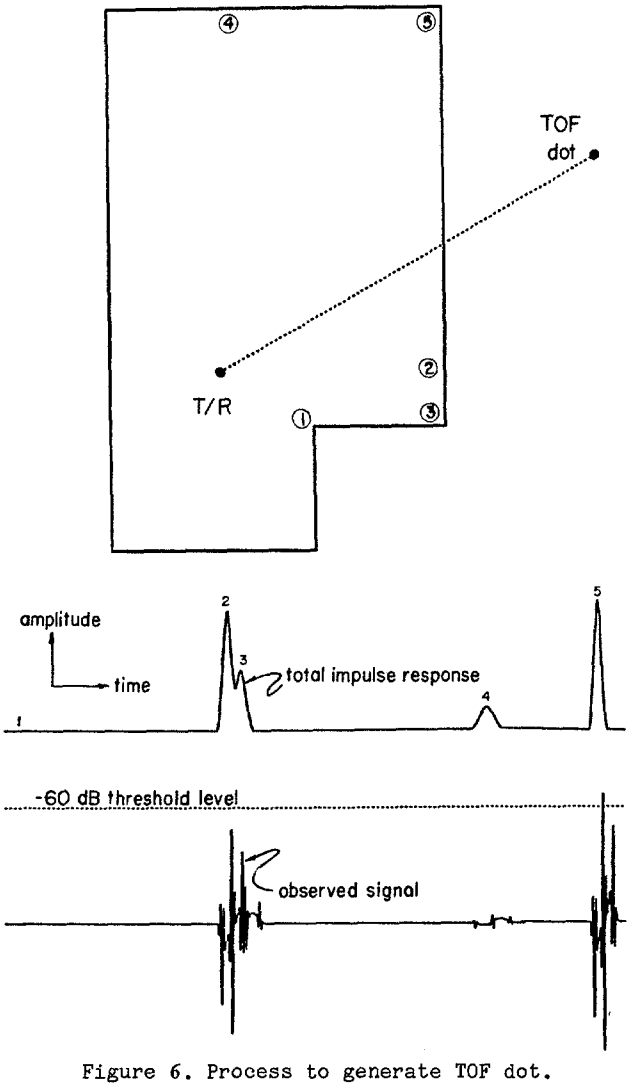

Figure 6. Process to generate TOF dot.

inclination θ. For an edge, the range also affects the amplitude of the reflection, as given by (4). The total impulse response is simply the sum of these individual responses and is shown in Fig. 6. The waveform observed at the output of the receiver is obtained by convolving the total impulse response with the pulse waveform. The result is shown in Fig. 6. A TOF range value is determined from the time that the detected signal exceeds the threshold value, which in the figure is set at -60 dB relative to the amplitude of a wall reflection at normal incidence. The TOF dot is placed at the appropriate range along the transducer line-of-sight as shown in Fig. 6. In the case shown in the figure, the signal reflected from the corner, marked 5, exceeds the threshold. By placing the dot along the line-of-sight, it is situated outside the space of the floor plan. This illustrates the problems mentioned earlier: 1) there is no physical object at the dot location, and 2) the wall marked 2, that lies along the path, is not detected.

It may be desirable to move the transducer around the interior space, as with a vehicular robot, or to examine the floor plan from different interior points. To do this efficiently, we code the floor plan in terms of the elements that are visible from any interior point, as described in the next section.

CODING THE FLOOR PLAN WITH VISIBELS

We propose to code the floor plan to indicate which reflecting elements (walls, corners and edges) are visible from any interior position. In our coding procedure, the floor plan is represented as a two dimensional grid, each member of which is represented by a positive integer, called a visibel. Each bit of the integer corresponds to a particular element in the floor plan, and is equal to 1, if the element is visible by the transducer from that position in the floor plan, or is equal to 0 otherwise. The members of the grid on the boundary of the floor plan, defined by the walls enclosing the interior space, are set to -1.

The quality of being visible depends on the particular element. A wall is detected only by the reflection that bounces directly back to the transducer. Hence, for a wall to be visible, the transducer location within the space must have an unobstructed line-of-sight that is perpendicular to some section of the wall. For corners and edges to be visible, the transducer must have an unobstructed line-of-sight to the point of intersection between the planes defining the element. In CEW world, it is an edge that blocks the visibility of another element.

The values of all the visibels covering the interior space are computed by exhaustively checking the visibility of each element at every grid location. This operation is performed as an initialization step in the simulation, immediately after the floor plan is specified. The signal generation phase of the simulation is then not burdened by determining the path of the reflected signals.

A region in the floor plan from which a particular element is not visible is called its shadow. Examples of shadow regions are shown in Fig. 7. In the shadow region of a particular element, the corresponding visibel bit value is zero.

Shadow regions for a wall are produced by edges that block the perpendicular projection. Those for a edge and a corner are produced by other edges that obstruct their direct line-of-sight by the transducer. The visible region for a wall is found by projecting it into the interior space and reducing the width of the projection monotonically as an obstructing edge is encountered. The boundary of the shadow region for a corner is defined by the line connecting the corner to the blocking edge. Unlike a corner, which can be viewed from only one quadrant, an edge can be viewed from three. The shadow region for an edge

is most easily generated by applying the corner shadow algorithm to the three quadrants of view. The shadow regions are determined by assuming the transducer aperture radius to be zero. This is reasonable if the room dimensions are large compared to those of the transducer, which is almost always the case in practice.

Having set the values of the visibels, the transducer can be positioned anywhere in the interior space and the sum of the impulse responses from all the visible elements lying within the transducer field-of-view contribute to the detected signal can be determined. In the next section, two examples of the sonar maps produced with our model will be presented.

SIMULATED SONAR MAPS

In this section, we present sonar maps that were generated with our model. When we introduce the transducer into the CEW world, we obtain the CEWT model. The parameters of the CEWT model are given in Table 1.

Table 1. CEWT Model Parameters

maximum floor plan area	1.28 x 1.28 m
grid size	128 x 128
element and transducer location resolution	1cm
sampling rate (f_s)	1 MHz
range resolution (sonic speed/$2f_s$)	0.17 mm

Polaroid transducer parameters:

resonant frequency	62 kHz
bandwidth (full width half max)	20 kHz
aperture radius	2 cm

To indicate the flexibility of the model, we also illustrate the effect of varying the threshold level. Sonar maps were generated with the threshold level set at -20 dB, relative to the amplitude observed from a normally incident wall. These are compared to sonar maps having the more sensitive threshold value equal to -40 dB. Most current sonar systems operate between these two values.

A floor plan is specified by placing corners, walls and edges at a set of locations in the grid defining the space, and the sonar map is generated by rotating the transducer in a complete circle and taking TOF readings every 2°. We consider two floor plans, designated CEW0 and CEW1. CEW0 is the simple case that serves to illustrate the steps in sonar map generation and is compared to an actual sonar map. CEW1 is more complicated and illustrates some of the subtle features of sonar map interpretation.

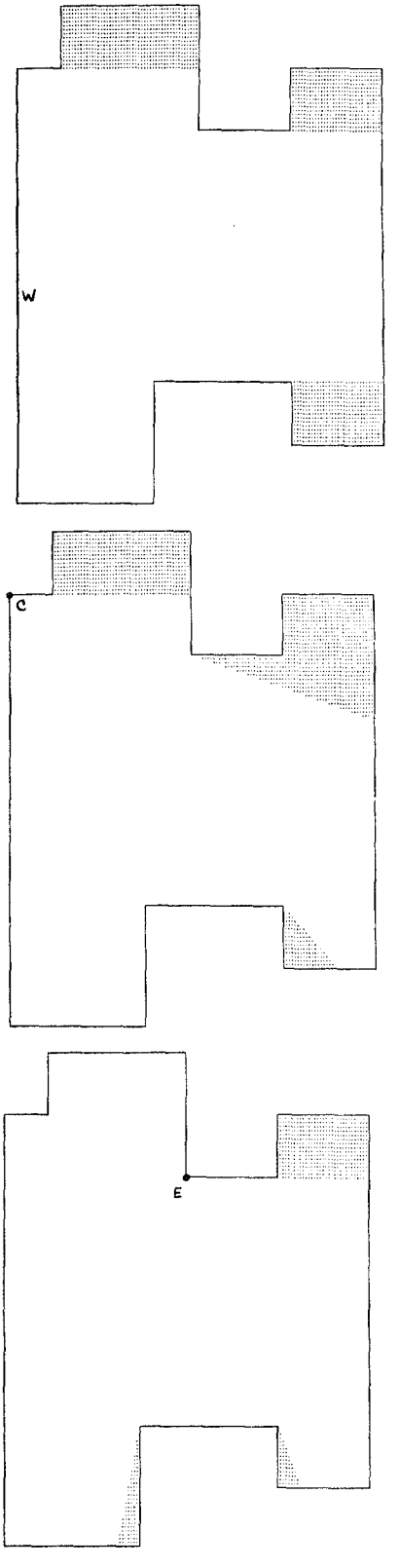

Figure 7. Shadows for wall W, corner C and edge E.

CEW0 Map. The CEW0 sonar map is shown in Fig. 8. The dashed lines indicate the true floor plan and the transducer/receiver location is denoted by the dot T/R near the center of the space. To verify the simulation model, actual sonar maps produced with the Polaroid sensor and using threshold values of -20 dB and -39 dB are shown in Fig. 9.

The following points from the sonar maps are noteworthy:

1) The equivalence of a wall and corner is evident from the identical TOF dot patterns that each produces.

2) The beam width of the transducer can be defined as the range of inclination angles over which a reflecting element generates a signal above the threshold level. Note that the beam width at the -20 dB threshold level is $\pm 6^{\circ}$ and increases to $\pm 12^{\circ}$ at the -40 dB level. Hence, there is a tradeoff between resolution (beam width) and sensitivity (threshold level).

3) The edge is not visible at the -20 dB threshold level, but becomes visible at the more sensitive -40 dB threshold level.

In addition to the patterns predicted by the model, the actual sonar map also shows the presence of multiple reflection artifacts [5], labeled m.r. in Fig. 9. The dashed line in Fig. 9 shows the path of the signal that is deflected by the wall and reflected by the corner, to produce the topmost m.r. artifact. The dot produced by the detected signal is, of course, placed at the appropriate range along the transducer line-of-sight, thus indicating a structure where none actually exists. Additional multiple reflection artifacts also exist, but are not shown in the figure because they lie at ranges that exceed the capacity of our analog-to-digital converter memory. These artifacts are not generated by our model, which considers only primary reflections, since their inclusion would greatly complicate the model. Our model does, however, accurately predict the behavior of the primary reflectors, when they are detected.

The sonar maps indicate the difficulty of doing the inverse problem, or determining the true floor plan from the TOF dot pattern. The inverse problem has not yet found a suitable answer, although the way to the solution may be guided by these simulation results.

CEW1 Map. The results of scanning CEW1 are shown in Fig. 10. The same observations made above are also true here, but an additional effect is also evident here. The TOF system returns the range of the first detected signal that exceeds the threshold level. Hence, it is possible that much larger reflected signals occurring at later times are not detected. This results is a shielding of some of the more remote elements by those more proximal. These are illustrated by the reflections from corner in the lower left of the CEW1 floor plan, that is shielded temporarily by the edge lying between it and the transducer. Because the amplitude of a reflection decreases as the transducer is rotated away from the reflecting element, the edge dots disappear and the corner dots reappear. These corner dots are isolated and can be interpreted as representing another element. This illustrates the confusion with the current interpretation of sonar maps.

SUMMARY AND CONCLUSIONS

This paper has described a simulation model for generating sonar maps that is based on the physical principles of sound propagation. The simulation considered a simple world model populated by reflecting elements consisting of corners, edges or walls, and the time-of-flight (TOF) system for range detection. An impulse response formulation was employed to determine the TOF reading when multiple reflecting elements are in the transducer field-of-view. To make this determination efficient, the floor plan was coded in terms of visibels, that indicate which elements are candidates for producing reflections. The sonar maps of two floor plans were generated to illustrate the subtle features in sonar map interpretation. Comparisons with actual sonar maps verified the validity of the model. The interesting points brought out by the model include:

1) From a single reflected signal, it is impossible to differentiate corners, edges and walls, since the forms of their impulse responses are identical.

2) Using the signals from a sector scan, time-of-flight dots form arcs in the map, since the dot is placed along the transducer line-of-sight, while the distance from the transducer to the reflecting element is constant. The length of the arc corresponds to the effective beam width and increases as the threshold level decreases. At the most sensitive threshold level considered (-40 dB relative to the amplitude observed from a normally incident wall), the elements that are close to the transducer can shield those at further ranges and cause confusion in the interpretation of the sonar map.

REFERENCES

[1] Moravec, H.P. and Elfes, A. High resolution maps from wide angle sonar. IEEE Intl. Conf. Robotics Automation, 1985, pp. 116-121.

[2] Crowley, J.L. Dynamic world modeling for an intelligent mobile robot using rotating ultrasonic ranging device. IEEE Intl. Conf. Robotics Automation, 1985, pp. 116-121.

[3] Tachi, S. and Komoriya, K. Guide dog robot, Second Intl. Symp. Robotics Res. Kyoto, 1984.

[4] Polaroid Corporation, Ultrasonic Range Finders, 1982.

-20dB Threshold:

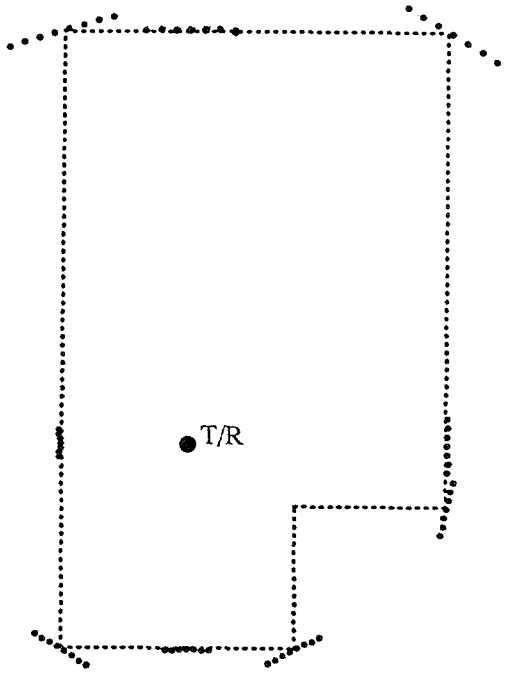

-20 dB Threshold:

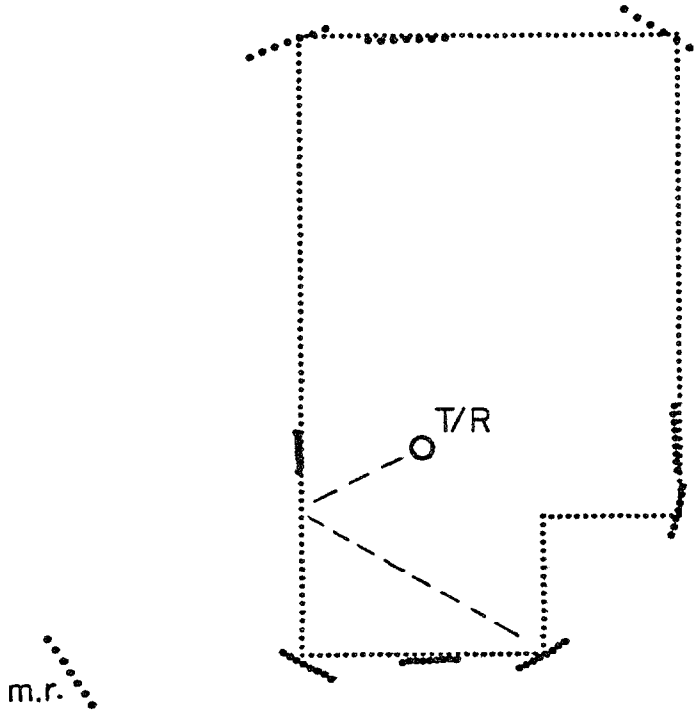

-40 dB Threshold:

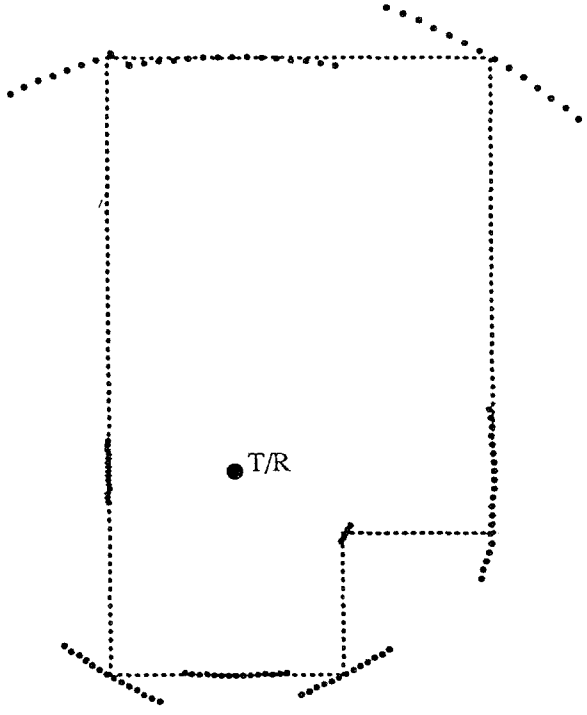

-39 dB Threshold:

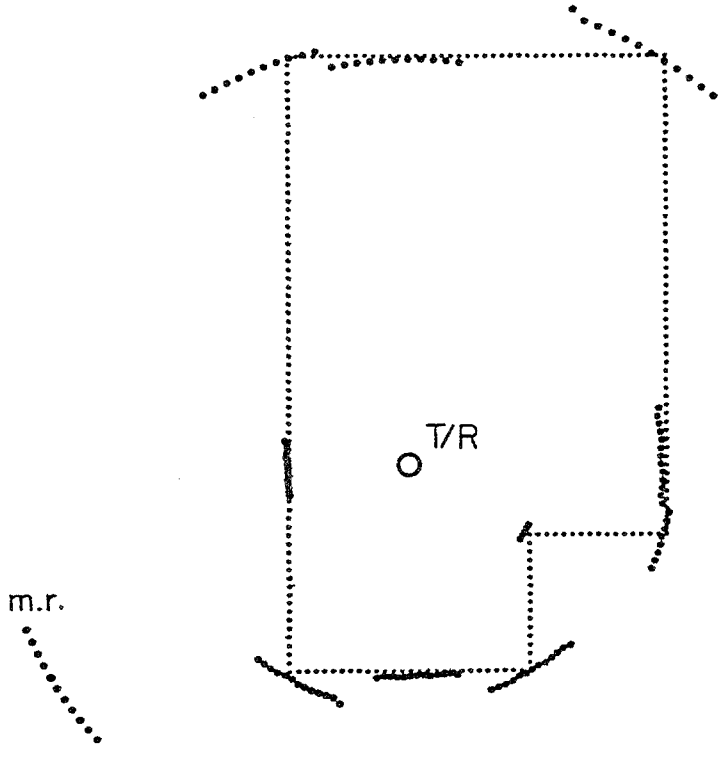

Figure 8. CEWO Simulation results.

Figure 9. Real sonar map.

-20 dB Threshold:

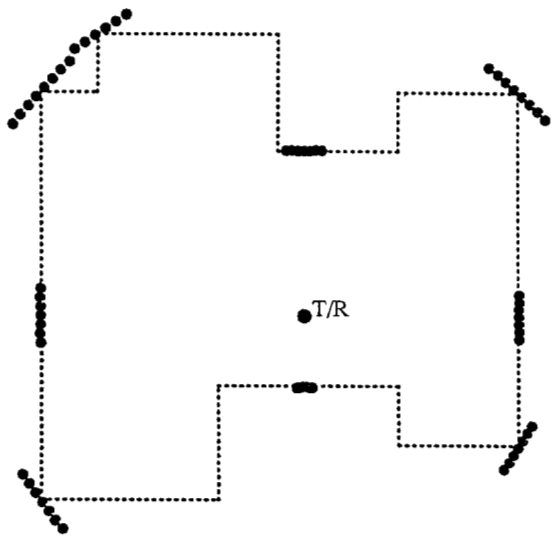

-40 dB Threshold:

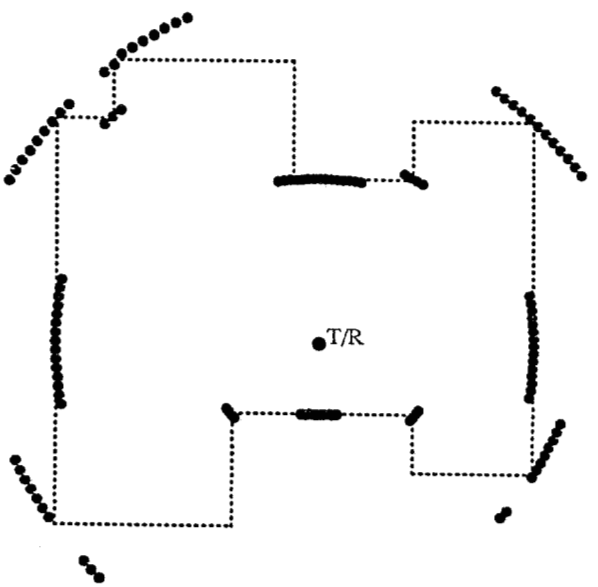

Figure 10. CEW1 Simulation results.

[5] Wells, P.N.T., Biomedical Ultrasonics, Academic Press, 1977.

[6] Kuc, R. and Siegel, M.W. Physically-based simulation model for acoustic sensor robot navigation. To appear in IEEE Trans. PAMI.

[7] Kuc, R. and Di, Y.D. Intelligent sensor approach to differentiating sonar reflections from corners and walls. Proc. Intl. Conf. Intel. Autonomous Sys., Amsterdam, 1986.

[8] Morse, P.M. and Ingard, K.U. Theoretical Acoustics, McGraw-Hill, 1968.